

AD-775 631

THE INTERACTION AND DAMAGE EFFECTIVE-
NESS OF TWO EXPANDING NON-SPHERICAL
EXPLOSION BUBBLES

Richard G. Leamon, et al

Naval Ordnance Laboratory
White Oak, Maryland

11 January 1974

DISTRIBUTED BY:

NTIS

National Technical Information Service
U. S. DEPARTMENT OF COMMERCE
5285 Port Royal Road, Springfield Va. 22151

AD 775631
NOLTR 73-102

NOL

**TECHNICAL
REPORT**

**THE INTERACTION AND DAMAGE EFFECTIVENESS OF TWO EXPANDING NON-SPHERICAL
EXPLOSION BUBBLES**

BY
Richard G. Leamon
Hans G. Snay

11 JANUARY 1974

NAVAL ORDNANCE LABORATORY
WHITE OAK, SILVER SPRING, MD. 20910

- Approved for public release; distribution unlimited

Reproduced by
NATIONAL TECHNICAL
INFORMATION SERVICE
U S Department of Commerce
Springfield VA 22151

DDC
RECEIVED
MAR 19 1974
RECEIVED
E

**NAVAL ORDNANCE LABORATORY
WHITE OAK, SILVER SPRING, MARYLAND 20910**

2

UNCLASSIFIED

NOLTR 73-102

11 January 1974

THE INTERACTION AND DAMAGE EFFECTIVENESS OF TWO EXPANDING NON-SPHERICAL EXPLOSION BUBBLES

This report is the second part of a study of the motion and mutual interaction of bubbles from two simultaneously initiated underwater explosions. The assumption of a spherical bubble shape, made in a previous technical report on this subject, NOLTR 73-101, is dropped and the change of the bubble shape is calculated.

This work was part of a quick-response program with a stringent deadline. In its initial phase it was supported by NAVORDSYS COM under Task ORD-332/001/092-1/UF/17-354-315. The time available in such crash programs is rarely sufficient to carry the study beyond the point where the questions can be answered with a fair degree of confidence. Once the deadline is met, often neither time nor funds are available to complete the problem and prepare a satisfactory publication. The generous support of NAVORDSYS COM under Tasks NOL-538/PMO-4021 and ORD 35C-501/092-1/UF33-351-504 made it possible to complete the calculations and to document the results of this study.

The authors appreciate the assistance of Mr. Charles G. Simpson who prepared the illustrations and reviewed the text.

ROBERT WILLIAMSON II
Captain, USN
Commander



C. J. ARONSON
By direction

UNCLASSIFIED
NOLTR 73-102

CONTENTS

	Page
1. INTRODUCTION	1
2. METHOD	2
2.1 The Velocity Potential	3
2.2 Equations for the Interface	5
2.3 Determination of $Q(t)$	6
2.4 Selection of Bubble Parameters and Initial Conditions	10
2.5 The Computer Program	12
2.6 Description of the MACYL Calculations	13
3. NUMERICAL CALCULATIONS	14
3.1 Present Method	14
3.2 MACYL Calculations	15
4. DAMAGE EFFECTIVENESS	16
4.1 Bubble Parameters Which Cause the Whipping of Ships	16
4.2 Damage Potential of Double Bubbles	20
4.3 Effectiveness of Interacting Bubbles	23
5. CONCLUSIONS	26
LIST OF REFERENCES	27

ILLUSTRATIONS

Figure	Title	Page
1	The Coordinate System	28
2	Sample Output of a Calculation Made Using the MACYL Computer Technique	29
3	Bubble Interfaces and Particle Paths for Double Explosion Bubbles Separated by 10.6 Charge Radii	30
4	Bubble Interfaces and Particle Paths for Double Explosion Bubbles Separated by 31.7 Charge Radii	31
5	Bubble Interfaces and Particle Paths for Double Explosion Bubbles Separated by 105.7 Charge Radii	32
6	Comparison of Calculations Made with Potential Flow Theory with Calculations by the MACYL Code	33
7	Explosion Geometry Below Target	34
8	Source Strength of Two Interacting Bubbles	35

REPORT DOCUMENTATION PAGE		READ INSTRUCTIONS BEFORE COMPLETING FORM
1. REPORT NUMBER NOLTR 73 102	2. GOVT ACCESSION NO.	3. RECIPIENT'S CATALOG NUMBER
4. TITLE (and Subtitle) THE INTERACTION AND DAMAGE EFFECTIVENESS OF TWO EXPANDING NON-SPHERICAL EXPLOSION BUBBLES		5. TYPE OF REPORT & PERIOD COVERED Final
7. AUTHOR(s) Richard G. Leamon Hans G. Snay		6. PERFORMING ORG. REPORT NUMBER NOLTR 73-102
9. PERFORMING ORGANIZATION NAME AND ADDRESS Naval Ordnance Laboratory White Oak, Silver Spring, Md. 20910		8. CONTRACT OR GRANT NUMBER(s)
11. CONTROLLING OFFICE NAME AND ADDRESS Naval Ordnance Systems Command Code 0350 Washington, D.C. 20360		10. PROGRAM ELEMENT, PROJECT, TASK AREA & WORK UNIT NUMBERS ORD 35C-501/092-1/UF33 351-504
14. MONITORING AGENCY NAME & ADDRESS (If different from Controlling Office) Same as above		12. REPORT DATE 11 January 1974
		13. NUMBER OF PAGES 35 40
		15. SECURITY CLASS. (of this report) Unclassified
		15a. DECLASSIFICATION/DOWNGRADING SCHEDULE
16. DISTRIBUTION STATEMENT (of this Report) Approved for public release; distribution unlimited		
17. DISTRIBUTION STATEMENT (of the abstract entered in Block 20, if different from Report) Same as above		
18. SUPPLEMENTARY NOTES None		
19. KEY WORDS (Continue on reverse side if necessary and identify by block number) Bubbles Underwater Explosions Multiple Explosions Underwater Explosion Bubbles Bubble Interactions Underwater Explosion Damage Whipping of Ships		
20. ABSTRACT (Continue on reverse side if necessary and identify by block number) The phenomena associated with the expansion of two bubbles resulting from the simultaneous underwater detonation of two equal charges are studied. Potential flow and incompressible medium are assumed for the calculation of the behavior and shape of the interacting bubbles. The results of this approximation compare favorably with		

UNCLASSIFIED

SECURITY CLASSIFICATION OF THIS PAGE(When Data Entered)

20 those obtained from a more sophisticated analysis using finite difference techniques (MACYL Code). The potential flow calculations are simple and require only a small portion of the machine time needed for the finite difference method.

An outline is given of the fundamentals of the whipping of ships. These processes are caused by the pulsating bubble of explosions beneath the bottom of ships and are capable of doing severe damage to a ship. It is concluded that double explosions do not offer advantages in the damage effectiveness beyond that of a single explosion of equal total weight.

UNCLASSIFIED

SECURITY CLASSIFICATION OF THIS PAGE(When Data Entered)

ia

THE INTERACTION AND DAMAGE EFFECTIVENESS OF TWO
EXPANDING NON-SPHERICAL EXPLOSION BUBBLES

1. INTRODUCTION

The underwater explosion of two simultaneously or sequentially initiated separated charges produces complex shock wave and bubble phenomena. The interaction of the two shock waves has been studied in the past^{1,2}. This report is a continuation of a study of the bubble phenomena of separated charges.

With two separated charges, two distinct bubbles are formed following the detonation. The bubbles will deform from a spherical shape as a result of the hydrodynamic interaction. The authors have shown³ that the centers of two spherical explosion bubbles remain essentially stationary during the expansion phase but later attract strongly as the bubble contracts. It is assumed that explosion bubbles which are not constrained to a spherical shape will behave in the same manner. The analysis deals with explosion bubbles that pulsate in phase. Only the expansion phase will be considered. The effect of buoyancy upon the bubbles is neglected.

Our study utilizes the methods of potential flow theory to describe the expansion of the bubbles and their shapes as a

¹ N. L. Coleburn and L. A. Roslund, "Collision of Spherical Shock Waves in Water," NOLTR 68-110, (1968)

² R. J. Seeger and H. Polachek, "On Shock Wave Phenomena: Waterlike Substances," Journal of Applied Physics, 22, 640 (1951)

³ R. G. Leamon, C. G. Simpson, and H. G. Snay, "The Interaction of Two Spherical Explosion Bubbles," NOLTR 73-101, (1973)

function of time. Lagrangian coordinates are used to follow individual particles on the bubble-water interface and for the determination of the shape of the bubble. This problem has been studied elsewhere using the far more sophisticated MACYL computer technique. The results of our approximation compare favorably with those obtained with the MACYL analysis that uses finite difference techniques. The potential flow calculations are simple and require only a small portion of the machine time needed for the finite difference method.

2. METHOD

In the method described below, a solution of the appropriate hydrodynamic equation--Laplace's equation--is used. Such a solution specifies the particle velocities in the water. The initial shape of each bubble and the equation of state for the water and that for the gaseous contents of the bubbles are those of the classic bubble theory, namely that of an incompressible medium for the water surrounding the bubbles and that of an ideal gas for the contents of the bubbles.

The bubble interface* is assumed to consist of the same particles of water throughout the pulsation. If the particle velocities in the water are known, and if the initial interface is specified, then the shape of the bubbles can be calculated as a function of time by following the motion of the interface particles. This approach allows the bubbles to combine or coalesce.

* For the purpose of this report, the term interface shall refer to the bubble-water interface regardless of whether or not the two bubbles are coalescent.

2.1 The Velocity Potential. For the purpose of describing the motion of the bubbles, the flow field in the water is taken to be irrotational and incompressible. These assumptions form the basis of the well-established bubble theory,^{4,5} the classic bubble theory. Under these conditions, a velocity potential, ϕ , exists which describes the flow field and which satisfies Laplace's equation

$$\nabla^2 \phi = 0 . \quad (2.1)$$

Any velocity potential which satisfies this equation is a possible solution to our problem. One class of functions which satisfy Equation (2.1) are called singular solutions, so called because ϕ becomes infinite at the origin of these solutions. These include sources, dipoles, quadrupoles, etc. The simplest of these solutions, the source, is written as

$$\phi = \frac{Q(t)}{r} , \quad (2.2)$$

where $Q(t)$ is an arbitrary function of time and r is the distance from the origin to any point in the flow field. In fact the source is the complete solution of a single pulsating non-migrating spherical bubble. In this case it takes the form

⁴ B. Friedman, "Theory of Underwater Explosion Bubbles," Institute of Mathematics and Mechanics, New York University, Report No. IMM-NYU 166, (1947). Reprinted in Underwater Explosion Research, Volume II, The Gas Globe, Office of Naval Research, p. 329-378, (1950)

⁵ H. G. Snay and E. A. Christian, "Underwater Explosion Phenomena: The Parameters of Non-Migrating Bubbles," NAVORD 2937, (1952)

$$-\phi = \frac{A^2 \dot{A}}{r}, \quad (2.3)$$

where A is the radius of the spherical bubble and \dot{A} , its time derivative which is the radial velocity of the bubble interface.

We use two equal source potentials fixed in the flow field to represent the motion due to the two bubbles. These bubbles are taken as being formed by equal, simultaneous underwater explosions. The effect of buoyancy on the bubbles is neglected. This effect is known to be small for a single bubble during the expansion phase⁶. In addition there are compelling reasons for omitting the effect of buoyancy*. Using the axisymmetric coordinate system shown in Figure 1, the form of the velocity potential becomes

$$-\phi = Q(t) \left(\frac{1}{r_1} + \frac{1}{r_2} \right) \quad (2.4)$$

or

$$-\phi = Q(t) \left(\frac{1}{\sqrt{x^2 + y^2}} + \frac{1}{\sqrt{(x+B)^2 + y^2}} \right),$$

Where B is the total separation distance between the two charges. Physically, this is analogous to superposing the two velocity potentials which, taken individually, would correctly represent a single bubble.

⁶ H. G. Snay, "Underwater Explosion Phenomena: The Parameters of Migrating Bubbles," NAVORD 4125, (1962)

* Compare with page 36 of reference 3

To first order we fix the location of the two sources at the initial separation distance of the two charges. The justification of this approach is provided by the previous study³ of the pulsation and migration of two interacting spherical bubbles. It was found that the centers of the interacting bubbles remain almost stationary* at first, but strongly move toward each other later as the bubble contracts. This assumption is further substantiated by the good agreement between calculations based on Equation (2.4) and calculations with the MACYL Code (See section 3.2).

2.2 Equations for the Interface. Since a bubble-water interface consists of the same particles throughout its motion**, the position of a particular point on the bubble interface can be determined by integration of the particle velocities over time.

The particle velocities for any point in the flow field are given by the gradient of the potential given by Equation (2.4),

$$u = - \frac{\partial \phi}{\partial x} \tag{2.5a}$$

$$u/Q(t) = \left(\frac{x}{r_1^3} + \frac{(x+B)}{r_2^3} \right)$$

$$v = - \frac{\partial \phi}{\partial y} \tag{2.5b}$$

$$v/Q(t) = y \left(\frac{1}{r_1^3} + \frac{1}{r_2^3} \right),$$

* In fact, the two equal spherical bubbles slightly repel one another, but the total distances moved are small.

** Vaporization or boiling of the ambient water into the bubble due to passage of the shock wave is ignored.

where u and v are the particle velocities in the x and y directions, respectively, as shown in Figure 1.

Thus, at any time t , the coordinates x and y of a point on the bubble interface are given by

$$x(t) = x(t_0) + \int_{t_0}^t u \, dt \tag{2.6a}$$

$$= x(t_0) + \int_{t_0}^t Q(t) \left(\frac{x}{r_1^3} + \frac{(x+B)}{r_2^3} \right) dt$$

and

$$y(t) = y(t_0) + \int_{t_0}^t v \, dt \tag{2.6b}$$

$$= y(t_0) + \int_{t_0}^t Q(t) y \left(\frac{1}{r_1^3} + \frac{1}{r_2^3} \right) dt,$$

where $x(t_0)$ and $y(t_0)$ are the coordinates of the interface particle at time t_0 . It is seen, then, that specifying $Q(t)$ is sufficient to find the motion of an interface particle. By tracing the trajectories of enough interface particles, it is possible to numerically determine the motion of the whole interface and obtain the resulting flow field.

2.3 Determination of $Q(t)$. The function $Q(t)$ may be determined from the equation for the conservation of energy.

The kinetic energy of the water is given by integration of the square of the velocities over the volume of the field.

$$\begin{aligned}
 T &= \frac{1}{2}\rho_0 \int_{\substack{\text{flow field} \\ \text{volume}}} \{u^2+v^2\} d\tau \\
 &= \frac{1}{2}\rho_0 \int_{\substack{\text{flow field} \\ \text{volume}}} \left\{ \left(\frac{\partial\phi}{\partial x}\right)^2 + \left(\frac{\partial\phi}{\partial y}\right)^2 \right\} d\tau .
 \end{aligned}
 \tag{2.7}$$

By use of Green's formula, this volume integral may be reduced to a surface integral enclosing the flow field volume. As there is no flow at infinite distance, the surface integral vanishes at infinity. This means that the surface integral needs to be taken over the bubble interface σ only. Thus, the kinetic energy in the flow field becomes

$$T = - \frac{1}{2}\rho_0 \int_{\substack{\text{bubble} \\ \text{interface}}} \left(\phi \frac{\partial\phi}{\partial n} \right) d\sigma ,
 \tag{2.8}$$

where $\partial\phi/\partial n$, the partial derivative of ϕ in the direction of the outward normal to the interface, is the normal velocity and ρ_0 is the density of the ambient water. Equation (2.8) can be expressed in terms of $Q(t)$ by use of Equations (2.5):

$$T = \frac{1}{2}\rho_0 Q^2(t) \int_{\substack{\text{bubble} \\ \text{interface}}} \left(\frac{1}{r_1} + \frac{1}{r_2} \right) \left[\left(\frac{u}{Q(t)} \hat{x} + \frac{v}{Q(t)} \hat{y} \right) \cdot \hat{n} \right] d\sigma ,
 \tag{2.9a}$$

where \hat{x} and \hat{y} are the unit vectors in the x and y directions and \hat{n} is the outward pointing unit vector normal to the bubble interface.

The expression in the square brackets is the dot product. For a single spherical bubble the kinetic energy becomes

$$T = 2\pi\rho_0 A^3 \dot{A}^2 = 2\pi\rho_0 Q^2 / A. \quad (2.9b)$$

The potential energy, Ω , of one of the two bubbles is given by

$$\Omega = P_0 V, \quad (2.10)$$

where P_0 is the hydrostatic pressure in the water and V is the volume of the bubble.

The gaseous contents of the bubbles are taken as ideal gases with a constant adiabatic exponent γ , an assumption carried over from the classic bubble theory. For each bubble, the internal energy of the gaseous bubble contents, G , is given by

$$G = P_r \left(\frac{V_r}{V} \right)^\gamma \frac{V}{(\gamma-1)}, \quad * \quad (2.11)$$

where P_r and V_r are arbitrary reference magnitudes, for instance the initial pressure and the corresponding initial volume.

The total energy of the mechanical system comprising the two bubbles and the surrounding water, $2E$, is conserved. Thus, the sum of the kinetic, potential, and internal energy is constant throughout the first pulsation. The magnitude E is called the bubble energy. For a single bubble, it is given by

$$T + \Omega + G = E \quad (2.12a)$$

or

* This equation holds only for two bubbles produced by the same explosive and charge weight. If the type of explosive or the charge weight is not the same, a different expression for G is required for each bubble. When such bubbles coalesce, their pressures may not be the same and a pressure equalization takes place at the moment of their combination.

$$T + P_o V + P_r \left(\frac{V_r}{V} \right)^\gamma \frac{V}{\gamma-1} = E. \quad (2.12b)$$

The desired expression for the source strength $Q(t)$ of one bubble may be obtained from Equations (2.12) and (2.9). At the instant t we have

$$Q(t) = \sqrt{(E-\Omega-G) / \frac{1}{2} \rho_o \int_{\text{bubble interface}} \left(\frac{1}{r_1} + \frac{1}{r_2} \right) \left[\left(\left(\frac{u}{Q(t)} \right) \hat{x} + \left(\frac{v}{Q(t)} \right) \hat{y} \right) \cdot \hat{n} \right] d\sigma}, \quad (2.13)$$

where the positive square root is used as the bubbles are expanding.

Equations (2.12) and (2.13) may be somewhat simplified by using non-dimensional coordinates due to Friedman⁴. The transform to dimensionless variables is based upon the bubble energy E . The length scale L and the time scale C are given as

$$L = (3E/4\pi P_o)^{1/3} \quad (2.14a)$$

$$= 1.7289 (\epsilon W/Z)^{1/3}$$

$$C = L(3\rho_o/2P_o)^{1/2} \quad (2.14b)$$

$$= 0.37331 (\epsilon W)^{1/3} Z^{-5/6},$$

where P_o is the hydrostatic pressure, W is the weight of one of the explosive charges, Z , the hydrostatic pressure expressed in feet of ambient water, and ϵ , the specific bubble energy in cal/gm. Introducing the dimensionless variables

$$\begin{aligned}
 \tilde{t} &= t/C \\
 \tilde{A} &= A/L \\
 \tilde{r} &= r/L \\
 \tilde{\sigma} &= \sigma/4\pi L^2 \\
 \tilde{V} &= V/ \frac{4\pi}{3} L^3 \\
 \tilde{Q} &= Q/L^2 (L/C) \\
 \tilde{T} &= T/2\pi\rho_0 L^3 \left(\frac{L}{C}\right)^2
 \end{aligned}
 \tag{2.14c}$$

we obtain from Equation (2.12)

$$\tilde{T} + \tilde{V} + k\tilde{V}^{(1-\gamma)} = 1,
 \tag{2.15}$$

where k is the dimensionless bubble parameter defined as

$$k = \left[\frac{P_r}{P_0} \tilde{V}_r^\gamma \frac{1}{(\gamma-1)} \right].
 \tag{2.16}$$

Now Equation (2.13) for dimensionless source strength Q becomes

$$\tilde{Q}(\tilde{t}) = \sqrt{ \left[(1-\tilde{V}-k\tilde{V}^{(1-\gamma)}) \int \left(\frac{1}{r_1} + \frac{1}{r_2} \right) \left[\left(\frac{\tilde{u}}{\tilde{Q}(\tilde{t})} \right) \hat{x} + \left(\frac{\tilde{v}}{\tilde{Q}(\tilde{t})} \right) \hat{y} \right] \cdot \hat{n} \right] d\sigma } .$$

bubble
interface

(2.17)

2.4 Selection of Bubble Parameters and Initial Conditions. In order to find $Q(t)$ and the position of the points of the interface by means of Equation (2.6), it is necessary to specify γ for the bubble contents, the initial interface shape, as well as P_r and V_r . These parameters have been the subject of considerable study.^{5,6}

The values of the adiabatic exponent γ for the gaseous contents of the bubble are known for several types of high explosives. If the dimensionless notation is used, the determination of P_r and V_r is tantamount to determining k (provided, of course, that γ and the depth are given). On the basis of experimental pressure measurements made using single TNT explosive charges, Arons⁷ gives the following expression for k ,

$$k = 0.0552 Z^{\gamma-1}. \quad (2.18)$$

Strictly speaking, this relation should not be used if the depth of explosion is greater than 1000 feet but this is not a serious limitation for our consideration.

Initially, the two bubbles are assumed to be spherical. Their radius can be determined from Equation (2.15). Just after detonation the dimensionless kinetic energy in the water \tilde{T} is very small. Further, the dimensionless volume \tilde{V} is also small. Equation (2.15) becomes

$$k \tilde{V}_0^{(1-\gamma)} \approx 1 \quad (2.19)$$

or

$$\tilde{V}_0 \approx k^{1/(\gamma-1)}.$$

The dimensionless initial radius, \tilde{A}_0 , may thus be obtained from \tilde{V}_0 as

$$\tilde{A}_0 = (k^{1/(\gamma-1)})^{1/3} \quad (2.20)$$

⁷ A. B. Arons, "Secondary Pressure Pulses Due to Gas Globe Oscillations in Underwater Explosions II. Selection of Adiabatic Parameters in the Theory of Oscillation," *Journal of the Acoustical Society of America*, 20, (1948). Reprinted in *Underwater Explosion Research*, Volume II, The Gas Globe, Office of Naval Research, (1950)

which is analogous to a similar expression in the classic incompressible theory for a single bubble*.

The time, t_0 , at which the bubbles are spherical is taken as $t_0=0$, i.e., the instant of detonation. Strictly speaking, any incompressible representation of explosion phenomena is not valid for times very shortly after detonation. For these short times, phenomena which are due to the compressibility of the surrounding water (i.e., the shock wave formation) are dominant. An incompressible theory cannot possibly be in accord with reality at these times. It is not surprising then that the radius given by Equation (2.20) does not correspond to the radius of the explosive charge; Equation (2.20) gives a radius about 70% too large. When the values for A_0 and k from Equations (2.18) and (2.20) are used to represent a single explosion bubble, the results for the maximum radius and period agree with experimental measurements to within a few percent. These calculations also yield histories of the bubble radius and the pressure in the water which agree favorably with experimental records. There is every reason to believe these initial conditions are also applicable to explosion bubbles from two separated charges.

2.5 The Computer Program. The developments discussed in Sections 2.2, 2.3, and 2.4 were written into a computer code which calculates the expansion of two non-spherical bubbles. The time integrations for the coordinates of the bubble interface, Equation (2.6), were done numerically. Several interface particle trajectories must be calculated so that at each time step the entire interface shape can be determined by interpolation. The bubbles are axisymmetric about

* See Equation (13) of reference 7.

the x-axis of Figure 1. This means that the particle trajectories in only one plane containing the axis of symmetry (e.g., the x - y plane of Figure 1) need be considered. The interpolations were done using sections generated by rotation of segments of parabolas in the x - y plane about the x-axis near the y-axis. The directrix of the parabolas selected was along the y-axis. Near the x-axis and the median plane (i.e., the plane equidistant from both charges) the directrix was taken along the x-axis. Thus, at each time step the volume of the bubbles and the surface integration of Equation (2.17) is then used to find $Q(t)$ at this time. This value of Q is then used in the quadratures of Equation (2.6) to find the new position of interface particles, etc. The time integrations were made using the FNOL3 computer program described in a report by Ferguson and Orlow⁸.

2.6 Description of the MACYL Calculations. The MACYL computer program⁹ is a technique for solving incompressible, viscous, two-dimensional, axially symmetric, initial-value fluid flow problems involving zero, one, or two free surfaces. The incompressible Navier-Stokes equations and the continuity equation, Equation (2.21), are solved by finite difference methods.

$$\frac{\partial V}{\partial t} + (V \cdot \text{grad})V = - \frac{1}{\rho} \text{grad } p + \frac{\eta}{\rho} \nabla^2 V$$

(2.21)

⁸ R. E. Ferguson and T. A. Orlow, "FNOL3, A Computer Program to Solve Ordinary Differential Equations," NOLTR 71-2, (1971)

⁹ J. E. Welch, F. H. Harlow, J. P. Shannon, B. J. Daly, "The MAC Method--A Computing Technique for Solving Viscous, Incompressible, Transient Fluid-Flow Problems Involving Free Surfaces," Los Alamos Scientific Laboratory, LA-3425, (1966)

$$\frac{\partial \rho}{\partial t} + \rho \operatorname{div} V + V \cdot \operatorname{grad} \rho = 0$$

where η is the dynamic viscosity. For details of the computing method see references 9 and 10. A sample of the MACYL output is shown in Figure 2. This figure shows the shape at the maximum expansion of a single bubble. The slight deviation from the spherical shape seen is due to the effect of gravity. The "scatter" of the points is typical of such calculations. It has been improved considerably since these calculations were made.

3. NUMERICAL CALCULATIONS

3.1 Present Method. Calculations were made assuming two 347-lb TNT charges with separations of 10, 30, and 100 ft exploding in a depth of 70 ft. The shapes of the interacting bubbles are illustrated in Figures 3, 4, and 5. Typically, 20 interface particle paths were considered. The figures show the trajectories of these particles. This number of interface paths gives agreement within 1% for the maximum radius and the half period of spherical bubbles. To obtain this check, the bubble pulsation was calculated by means of the classical theory (incompressible fluid) for charge weights of 347-lb TNT and 694-lb TNT.

The initial conditions and the important magnitudes associated with these calculations were as follows:

¹⁰ J. W. Pritchett, "MACYL--A Two-Dimensional Cylindrical Coordinate Incompressible Hydrodynamic Code," Naval Radiological Defense Laboratory USNRDL-LR-67-97, (1967)

Depth of Explosion	D = 70 ft
Isentropic Exponent	$\gamma = 1.2415$
Bubble Parameter	$k = 0.0552 z^{\gamma-1}$ = 0.16906
Bubble Energy	$\epsilon = 490 \text{ cal/gr}$
Length Scale Factor	$L = 1.7289 (\epsilon W/Z)^{1/3}$
W = 347-lb TNT	= 20.433 ft
W = 694-lb TNT	= 25.744 ft
Time Scale Factor	$C = 0.37331 (\epsilon W)^{1/3} z^{-5/6}$
W = 347-lb TNT	= 0.4347 sec
W = 694-lb TNT	= 0.5477 sec
Initial Radius	
Dimensionless	$\tilde{A}_0 = A_0/L = k^{1/3}(\gamma-1) = 0.08599$
W = 347-lb TNT	$A_0 = 1.7570 \text{ ft}$
W = 694-lb TNT	$A_0 = 2.2137 \text{ ft}$
Initial Pressure	$P(A_0) = 17,426.6 \text{ psi}$

Single Spherical Charge:

	Maximum Radius	Half Period*
W = 347-lb TNT	19.096 ft	0.327 sec
W = 694-lb TNT	24.06 ft	0.412 sec

3.2 MACYL Calculations. The results of calculations using the method in this report were compared with the calculations using the MACYL Code. Figure 6 illustrates the agreement between these two techniques. This figure is drawn for a charge separation of 10 ft and for two 347-lb TNT charges. The method starts with the same

* Half period is the time of the bubble maximum.

initial conditions as those used in our calculations. Agreement between the two methods for the expansion phase of the double bubble is seen to be within 10%.

4. DAMAGE EFFECTIVENESS

4.1 Bubble Parameters Which Cause the Whipping of Ships. It was originally believed that a double charge arrangement would produce greater damage to naval targets than a single charge of equal total weight. The analysis presented here has shown that this is not the case. In this paragraph, we present a summary of the considerations which originally led to this assumption. Subsequently, in paragraph 4.3, it will be shown that the results of the present study on the behavior of double bubbles invalidates the basis for this assumption.

Since we are dealing with bubble phenomena, an underbottom attack against surface ships is considered, as this is the most important type of damage done by the underwater explosion bubble. In this case, the explosion is set off at some distance below the bottom of the ship. The expanding bubble excites violent transverse flexural vibrations of the entire body of the ship, known as whipping. These vibrations almost always occur in the vertical plane, i.e., they are up-and-down motions.

The ship may be visualized as a floating beam (a girder) of varying cross section. The dangerous effects of whipping arise from the different acceleration of the sections of the ship. The section above the explosion is accelerated upward most strongly. The acceleration decreases with increasing longitudinal distance from

the attacked section. This uneven acceleration produces a bending of the ship and induces strong flexural oscillations¹¹ which can severely impair the girder strength of the ship and may even sever the ship into two parts.

An explosion beneath the ship produces rapid motions of the surrounding water. This flow exerts hydrodynamic forces on the ship which are proportional to the average vertical acceleration \dot{u} of the water displaced by the ship. These forces produce an upward acceleration \ddot{y} of the ship as well as elastic or plastic restraining forces in its structure.

Consider sections of the ship, each bounded by planes perpendicular to the ship's axis. For the i -th section we have:

$$\left(m_{Di} + m_{Wi}\right) \dot{u}_i = \left(m_i + m_{Wi}\right) \ddot{y}_i - F_i, \quad (4.1)$$

where

\dot{u}_i = average upward acceleration of the water which, in the absence of the ship, would occupy the space displaced by the i -th section

\ddot{y}_i = bodily upward acceleration of the i -th section

F_i = total of the restraining forces acting on both faces of the i -th section

m_{Di} = mass of water displaced by the i -th section

m_{Wi} = added mass of the i -th section = mass of water which appears to move with the section. m_{Wi} depends on the

¹¹ A. N. Hicks, "The Elastic Theory of the Explosion Induced Whipping Motion of Ships and Submarines" NCRE/R.532, (1968)

underwater shape of the section

m_i = actual mass of the i -th section = mass of hull, decks, bulkheads, stiffeners, machinery, etc. situated in the section.

Note that commonly

$$m_{Di} \neq m_i, \quad (4.2)$$

whereas according to Archimedes' principle

$$\sum_{i=1}^N m_{Di} = \sum_{i=1}^N m_i, \quad (4.3)$$

where N is the total number of sections.

The average upward acceleration \dot{u} due to the expansion of a spherical bubble of radius $A(t)$ is given by

$$\dot{u}_i = \frac{d_i}{r_i^3} \frac{d}{dt} \{A^2 \dot{A}\}, \quad (4.4)$$

where

d_i = depth of bubble center below the center of m_{Di}

r_i = slant distance between these centers.

Equation (4.4) holds for the case where the bubble center is on vertical plane of symmetry. The general case can be readily written down but is not of interest here.

The magnitude $A^2 \dot{A}$ is the source strength $Q(t)$ discussed in section 2 of this paper. It may thus appear that $Q(t)$, or specifically $\dot{Q}(t)$, is the physical magnitude responsible for the excitation

of whipping. Here further details of the whipping process must be considered before drawing a conclusion.

Equation (4.4) for the upward acceleration \dot{u} is based on the relations of incompressible fluid motion. As stated in paragraph 2.3 the assumption of an incompressible medium is adequate for the description bubble phenomena except for the early times following the instant of detonation. This exception holds for the whipping process to an even greater degree. At these early times, the target is subjected to the impact of the shockwave and its afterflow. At this stage Equations (4.1) and (4.4) lose their physical meaning and hence their validity.

The shockwave produces elastic or plastic deflections of the hull of the ship. The energy thus transmitted to the plating is either expended in the process of hull rupture or, if no rupture occurs, is transmitted to the side of the hull and the transverse bulkheads. Equalization of the upward momentum imparted by the shockwave into the members of the ship's structure ultimately yields upward motions of the sections of the ship that are analogous to whipping motions. These motions are enhanced by the afterflow of the shockwave, i.e., the flow caused by the expanding bubble. An analytic description of these early processes is difficult and has not yet been accomplished.

Whipping theory utilizes an approximation for these early phases which, judging from the good agreement between experimental and calculated results, seems to describe the actual phenomena very well. It is assumed that initially a velocity is imparted to the ship that corresponds to the maximum rate of the volume expansion of the bubble,

hence

$$\dot{y}_1(t=0) = \frac{m_{D1} + m_{W1}}{m_1 + m_{W1}} \frac{d_1}{r_1^3} \left(A^2 \dot{A} \right)_{\max}, \quad (4.5)$$

whereby

$$y_1(t=0) = 0. \quad (4.6)$$

Here $y_1(t)$ is the deflection of the axis of the ship at the center of the i -th section. The magnitude $\left(A^2 \dot{A} \right)_{\max}$ is the maximum source strength Q_{\max} .

It appears from Equation (4.5) that every section of the ship is decelerated for $t > 0$. This is because $\dot{y}_1(t=0)$ and Q_{\max} are maximum values and, hence $\dot{y}_1(t)$ and $Q(t)$ must subsequently decrease. For the same reason \ddot{y}_1 in Equation (4.1) as well as \dot{Q} are negative for $t > 0$. It is thus seen that the basic equation of the whipping theory (4.1) considers the retardation of the whipping velocity from its initial "kick-off velocity", $\dot{y}_1(t=0)$. Although this retardation is important for details of the whipping process, it appears that Q_{\max} is the parameter of predominant importance for whipping damage.

To summarize, the maximum source strength Q_{\max} is the primary measure of whipping damage which an expanding explosion bubble can inflict to a ship. The negative values of \dot{Q} that occur after Q_{\max} are parameters of secondary significance. The smaller $|Q|$, the less decelerated is the whipping motion and the larger is the damage under otherwise equivalent conditions.

4.2 Damage Potential of Double Bubbles. Figure 7 illustrates the superposition of the velocities produced by the expansion of two separate bubbles. As stated above, the velocity components from

each bubble are proportional to the source strength of each bubble $Q_j = A_j^2 \dot{A}_j$, $j = 1, 2$. To obtain a simple representation of Q we set

$$A(t) = JW^{1/3}Z^{-1/3}F_1(\tau) \quad (4.6)$$

$$t = \tau KW^{1/3}Z^{-5/6} \quad (4.7)$$

and

$$\dot{A}(t) = \frac{J}{K} Z^{1/2} F_2(\tau), \quad (4.8)$$

whence

$$A^2 \dot{A} = \frac{J^3}{K} W^{2/3} Z^{-1/6} F_3(\tau), \quad (4.9)$$

and

$$\frac{dA^2 \dot{A}}{dt} = \frac{J^3}{K^2} W^{1/3} Z^{2/3} F_4(\tau). \quad (4.10)$$

Here

J = Radius Coefficient

K = Period Coefficient

W = Charge Weight

Z = Hydrostatic Head.

The functions $F_1 \dots F_4$ are virtually independent of charge weight, depth, or the type of the explosive, but depend on the dimensionless time τ only. The trend of these functions is not important for our study.

According to Figure 7, the resultant upward velocity u from two separated bubbles generated by the simultaneous explosion of charges having the weights W_1 and W_2 is

$$u = \frac{J^3}{K} \frac{\sin\theta}{R^2} Z^{-1/6} \left[F_3(\tau_1) W_1^{2/3} + F_3(\tau_2) W_2^{2/3} \right], \quad (4.11)$$

or for equal charge weights with $W = W_1 = W_2$ and with $R = D/\sin\theta$

$$u = \frac{J^3}{K} \frac{\sin^3\theta}{D^2} Z^{-1/6} F_3(\tau) W^{2/3} \times 2. \quad (4.11a)$$

The magnitudes θ , D , and R are shown in Figure 7. If the two charges are combined into one single charge, we obtain

$$u = \frac{J^3}{K} Z^{-1/6} F_3(\tau) (W_1 + W_2)^{2/3} / D^2 \quad (4.12)$$

or if W_1 and W_2 are equal

$$u = \frac{J^3}{K} Z^{-1/6} F_3(\tau) W^{2/3} 2^{2/3} / D^2. \quad (4.12a)$$

Hence the resultant velocity u from two equal separated bubbles is $\sin^3\theta \times 2/2^{2/3}$ times larger than that from a lumped charge of equal total weight measured at the same distance. This corresponds to a 26% increase if θ is close to 90° .

For the acceleration \dot{u} , one finds

$$\dot{u} = \frac{J^3}{K^2} \frac{\sin\theta}{R^2} Z^{2/3} \left[F_4(\tau_1) W_1^{1/3} + F_4(\tau_2) W_2^{1/3} \right], \quad (4.13)$$

or for equal charge weights

$$\dot{u} = \frac{J^3}{K^2} \frac{\sin^3 \theta}{D^2} Z^{2/3} F_4(\tau) W^{1/3} \times 2. \quad (4.13a)$$

For a lumped charge we have

$$\dot{u} = \frac{J^3}{K^2} \frac{Z^{2/3}}{D^2} F_4(\tau) (W_1 + W_2)^{1/3} \quad (4.14)$$

or for equal charges W_1 and W_2

$$\dot{u} = \frac{J^3}{K^2} \frac{Z^{2/3}}{D^2} F_4(\tau) W^{1/3} \times 2^{1/3}. \quad (4.14a)$$

Here the acceleration \dot{u} from two equal separated bubbles is $\sin^3 \theta \times 2/2^{1/3} = \sin^3 \theta \times 1.59$ times larger than that from a lumped charge of total equal weight.

This possible enhancement of almost 60% originally stimulated the study described in this paper. It was quickly recognized that not the acceleration \dot{u} but the maximum velocity u_{\max} must be used as a criterion for the effectiveness. This decreased the maximum enhancement to 26%, which would still be a welcome gain.

This enhancement is obtained if the two bubbles move independently and do not interact. If interaction takes place a reduction of the enhancement must be expected since the greatest interaction corresponds to a combination into a single bubble. No enhancement occurs in this case.

4.3 Effectiveness of Interacting Bubbles. The interaction of two bubbles is the subject of our paper. Figure 8 shows the source strength Q for one of the two bubbles as a function of time. The charge arrangements consist of two 347-lb spherical TNT charges at 10-, 30-, and 100-ft separation. Also shown is the source

strength for a non-interacting bubble (infinite separation). Since the charge radius of a 347-lb charge is roughly one foot, the curves may also be used for other charge weights by expressing the separation in charge radii. More accurately, the curves hold for 10.6, 31.7, and 105.7 TNT charge radii.

Figure 8 illustrates that the interaction of the two bubbles reduces the maximum source strength, but increases the half period. Even at the large separation of 100 ft, a substantial interaction is noticeable. For a 10-ft separation, the interaction has increased so much that the maximum source strength is reduced to that of a lumped charge, shown by the dashed curve in Figure 8.

The dashed curve in Figure 8 is obtained as follows: The solid curves show the source strength Q for one of the two interacting bubbles. Being symmetric the other bubble produces the same Q , so that the total strength is $2Q$. If the separation B is reduced to zero a lumped charge of 694-lb TNT is obtained. Its total source strength is $2Q$ in our notation. To be consistent with the curves of Figure 8, we have shown $\frac{1}{2}Q(694 \text{ lb})$ for the source strength of the lumped charge.

The source strength Q is proportional to the square of the length scale, which in turn is proportional to the cube root of the bubble energy or the charge weight. This is seen from the definition of the dimensionless source strength \tilde{Q} given in Equation (2.14c). (Note that the time scale factor C is proportional to the length scale factor L . Hence, C/L which occurs in the definition of \tilde{Q} is independent of the charge weight.) It follows that

$$\frac{1}{2}Q(694 \text{ lb}) = \frac{1}{2} 1.5874Q(347 \text{ lb}) = 0.7937Q(347 \text{ lb}).$$

Since the dashed curve of Figure 8 refers to a single explosion, it can be compared with the curve for infinite separation which corresponds to $Q(347 \text{ lb})$. Therefore, the ordinates of the dashed curve are 79.37% of those of $Q(347 \text{ lb})$, whereas its time scale is $2^{1/3} = 1.25992$ larger.

If one adopts the maximum source strength as a measure of the severity of whipping damage, it is seen that no advantage in damage effectiveness is apparent for a double charge of ten-foot separation: For $\sin\theta = 1$, the resultant maximum upward velocity is just equal to that produced by a lumped charge. One may even argue that separated charges are inferior because in practical applications $\sin\theta$ is less than unity. This argument holds particularly true for the 30-ft or 100-ft separation. If the normal standoff from the ship's bottom is 30 ft, we have $\theta = 63.4^\circ$ and $\sin^3\theta = 0.7155$ for 30-ft charge separation and $\theta = 31.0^\circ$ and $\sin^3\theta = 0.1362$ for 100-ft separation. In both cases the term $\sin^3\theta$ more than compensates for the increase of Q_{\max} shown in Figure 8, which is 8% for 30-ft and 19% for 100-ft separation.

In the above considerations the resultant velocity on the perpendicular bisector is considered. In actuality, the velocity distribution along the ship must be taken into account. Here multiple charges have the advantage that the velocity decreases less from its maximum value. Hence, the velocity profile along the bottom of the ship is fuller for multiple charges than for a single charge. But a single charge usually produces a higher maximum velocity on the normal bisector.

This effect can only be accounted for by means of whipping calculations. Such a study has been completed at the Naval Ordnance Laboratory and it has confirmed the conclusion of the present study that no advantages can be expected from multiple charges in doing whipping damage to ships. These calculations will be described in a forthcoming paper.

5. CONCLUSIONS

We have demonstrated that potential flow theory using a single stationary point source of variable strength is sufficient for the calculation of the shape and the properties of two interacting bubbles during the expansion phase. The results of our simple calculations agree within 10% with those obtained by finite difference methods using the MACYL computer technique. The justification for assuming a stationary (not translating) point source is given by the results of our previous study³, which show that the centers of spherical bubbles expanding in unison remain essentially stationary. Upon contraction (not considered here) the centers move rapidly toward each other.

The maximum strength of the source representing the expanding bubble is a measure for the degree of whipping damage done by the bubble.

The interaction between two expanding bubbles reduces the maximum source strength even for large separations of bubble centers. As a consequence, double explosions offer no advantages in bubble damage effectiveness against ships.

REFERENCES

1. N. L. Coleburn and L. A. Roslund, "Collision of Spherical Shock Waves in Water," NOLTR 68-110, (1968)
2. R. J. Seeger and H. Polachek, "On Shock Wave Phenomena: Waterlike Substances," Journal of Applied Physics, 22, 640 (1951)
3. R. G. Leamon, C. G. Simpson, H. G. Snay, "The Interaction of Two Spherical Explosion Bubbles," NOLTR 73-101, (1973)
4. B. Friedman, "Theory of Underwater Explosion Bubbles," Institute of Mathematics and Mechanics, New York University, Report No. IMM-NYU 166, (1947). Reprinted in Underwater Explosion Research, Volume II, The Gas Globe, Office of Naval Research, p. 329-378, (1950)
5. H. G. Snay and E. A. Christian, "Underwater Explosion Phenomena: The Parameters of Non-Migrating Bubbles," NAVORD 2937, (1952)
6. H. G. Snay, "Underwater Explosion Phenomena: The Parameters of Migrating Bubbles," NAVORD 4125, (1962)
7. A. B. Arons, "Secondary Pressure Pulses Due to Gas Globe Oscillations in Underwater Explosions II. Selection of Adiabatic Parameters in the Theory of Oscillation," Journal of the Acoustical Society of America, 20, (1948). Reprinted in Underwater Explosion Research, Volume II, the Gas Globe, Office of Naval Research, (1950)
8. R. E. Ferguson and T. A. Orlow, "FNOL3, A Computer Program to Solve Ordinary Differential Equations," NOLTR 71-2, (1971)
9. J. E. Welch, F. H. Harlow, J. P. Shannon, B. J. Daly, The MAC Method--A Computing Technique for Solving Viscous, Incompressible, Transient Fluid-Flow Problems Involving Free Surfaces," Los Alamos Scientific Laboratory, LA-3425, (1966)
10. J. W. Pritchett, "MACYL--A Two-Dimensional Cylindrical Coordinate Incompressible Hydrodynamic Code," Naval Radiological Defense Laboratory USNRDL-LR-67-97, (1967)
11. A. N. Hicks, "The Elastic Theory of the Explosion Induced Whipping Motion of Ships and Submarines" NCRE/R.532, (1968)

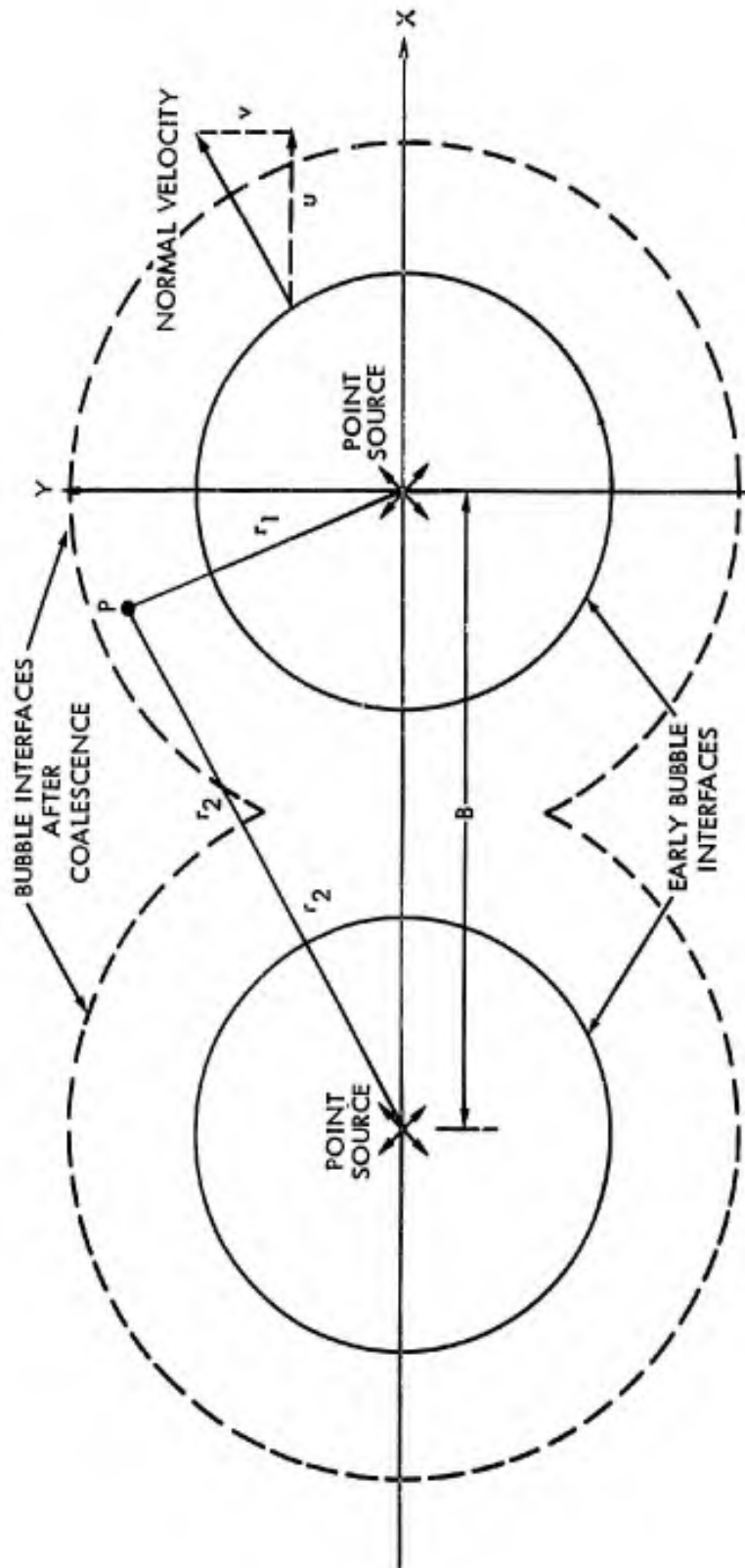


FIG. 1 THE COORDINATE SYSTEM

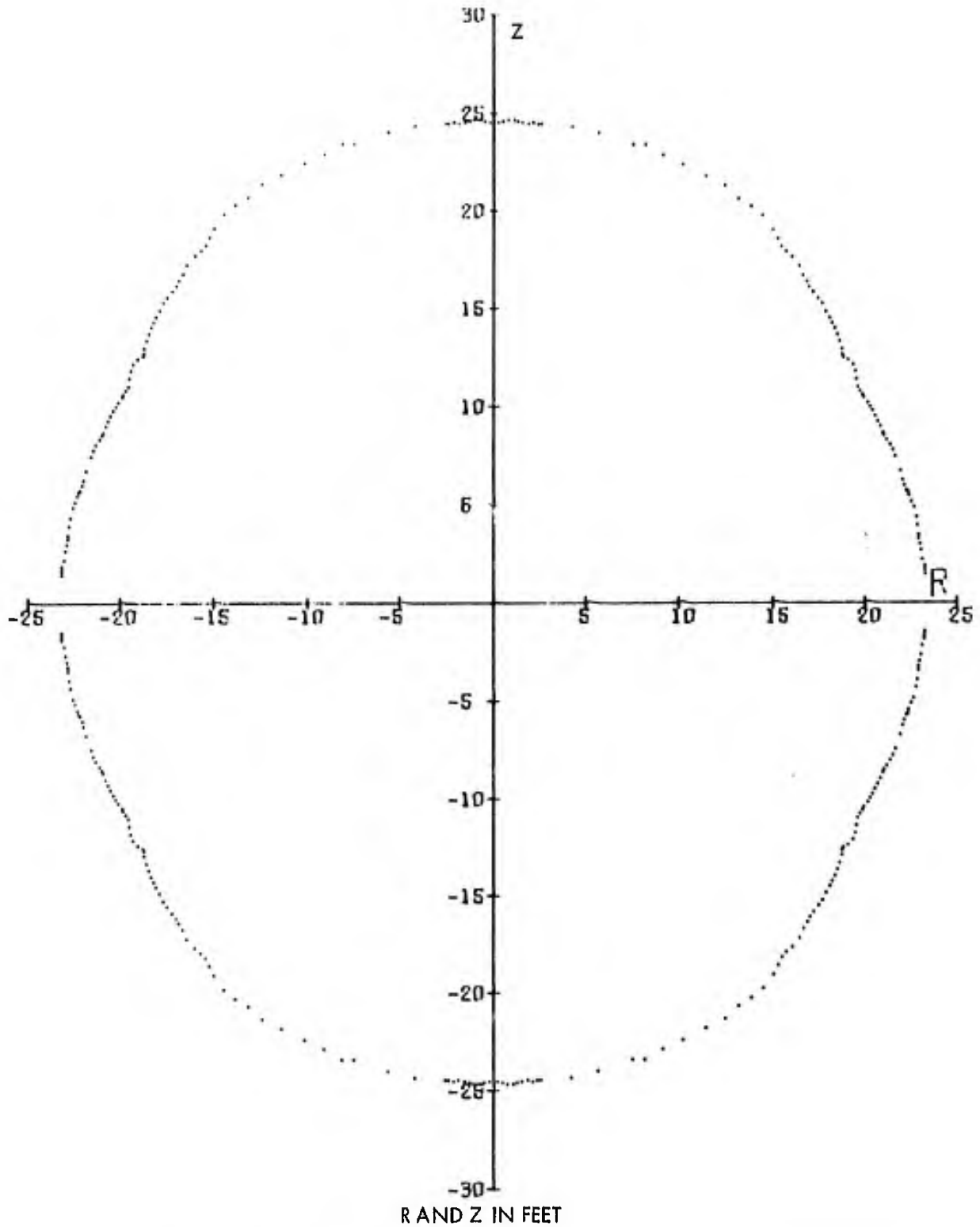


FIG. 2 SAMPLE OUTPUT OF A CALCULATION MADE USING THE MACYL COMPUTER TECHNIQUE

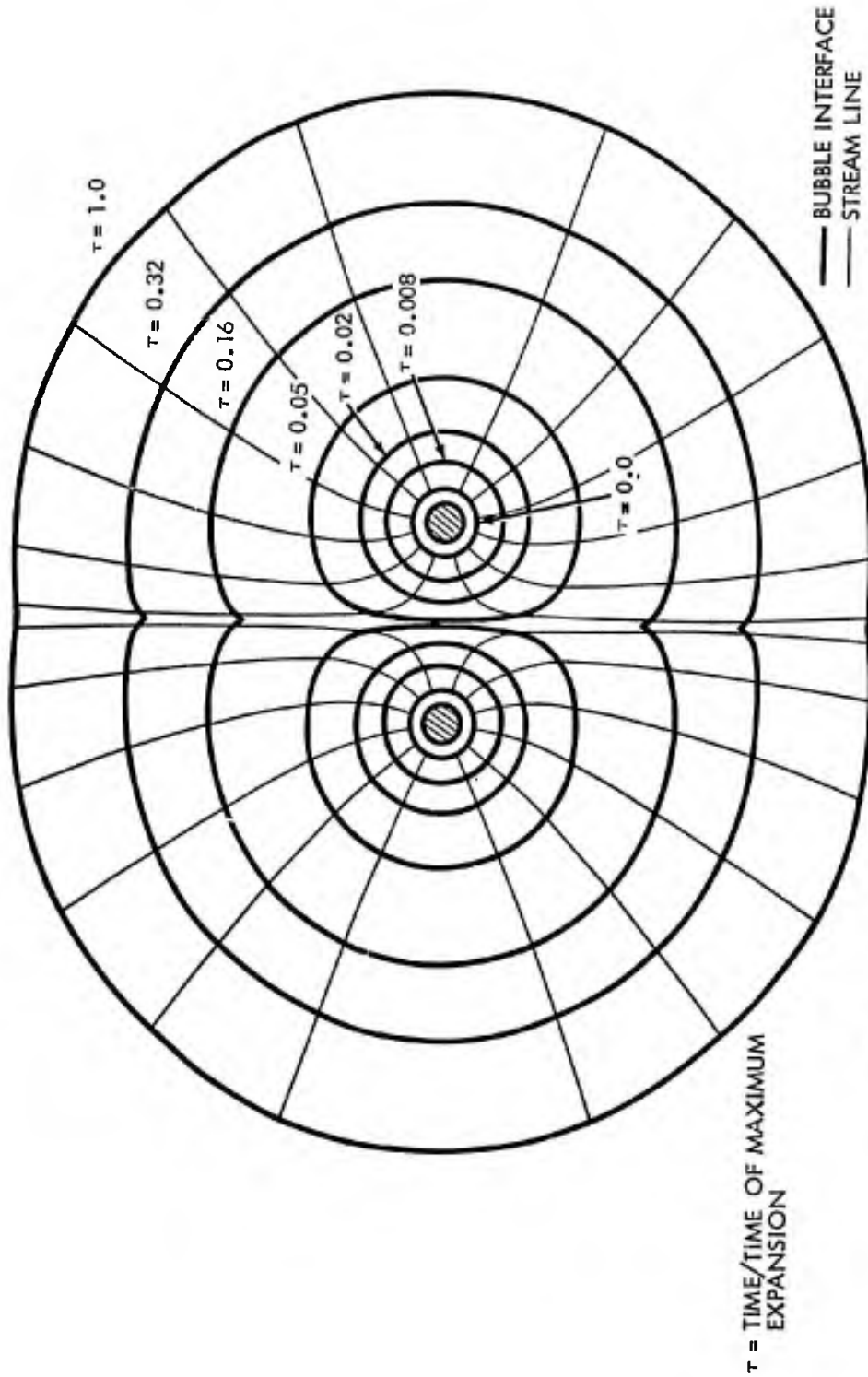


FIG. 3 BUBBLE INTERFACES AND PARTICLE PATHS FOR DOUBLE EXPLOSION BUBBLES SEPARATED BY 10.6 CHARGE RADII

The Calculations Were Made For An Explosion Of Two 347-lb TNT Charges 10 Feet Apart At A Depth Of 70 Feet. Coalescence Occurs Between The Reduced Time Of 0.05 And 0.16.

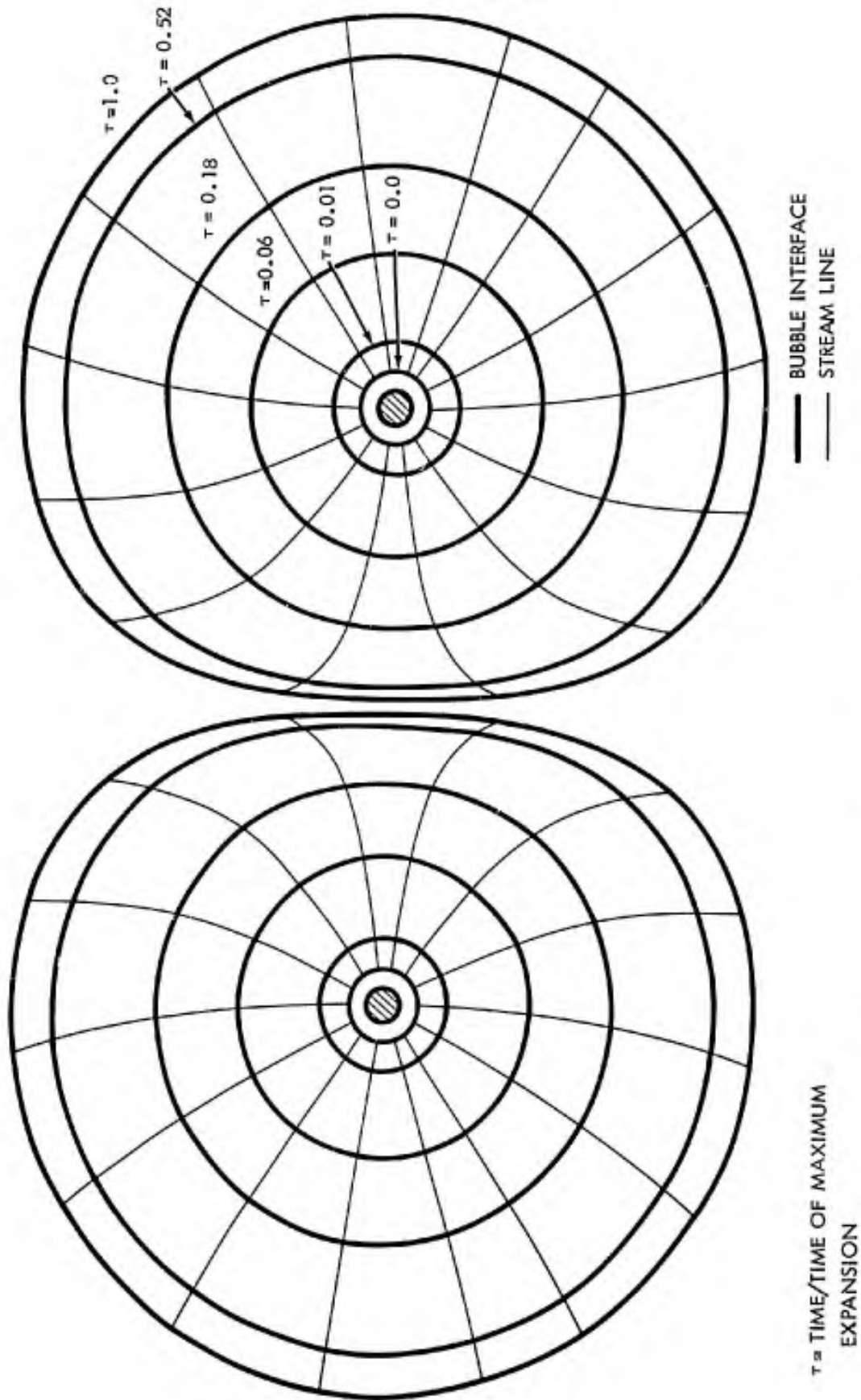


FIG. 4 BUBBLE INTERFACES AND PARTICLE PATHS FOR DOUBLE EXPLOSION BUBBLES SEPARATED BY 31.7 CHARGE RADII

The Calculations Were Made For An Explosion Of Two 347-lb Charges 30 Ft. Apart At A Depth Of 70 Ft.

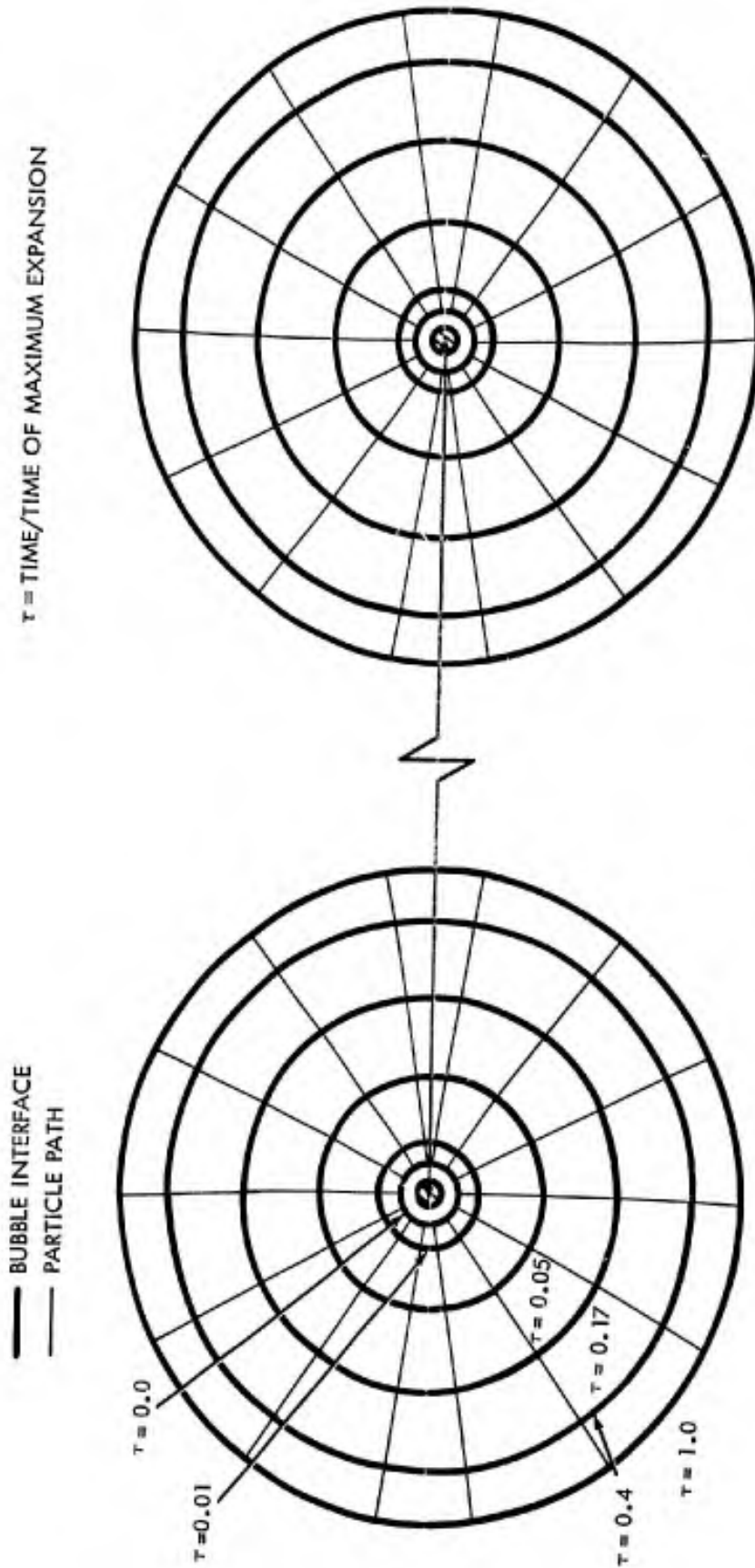


FIG. 5 BUBBLE INTERFACES AND PARTICLE PATHS FOR DOUBLE EXPLOSION BUBBLES SEPARATED BY 105.7 CHARGE RADII

The Calculations Were Made For An Explosion Of Two 347-lb TNT Charges At A Depth Of 70 Feet. Despite The Relatively Large Separation And The Almost Spherical Appearance, These Bubbles Interact Noticeably As Seen In Fig. 8.

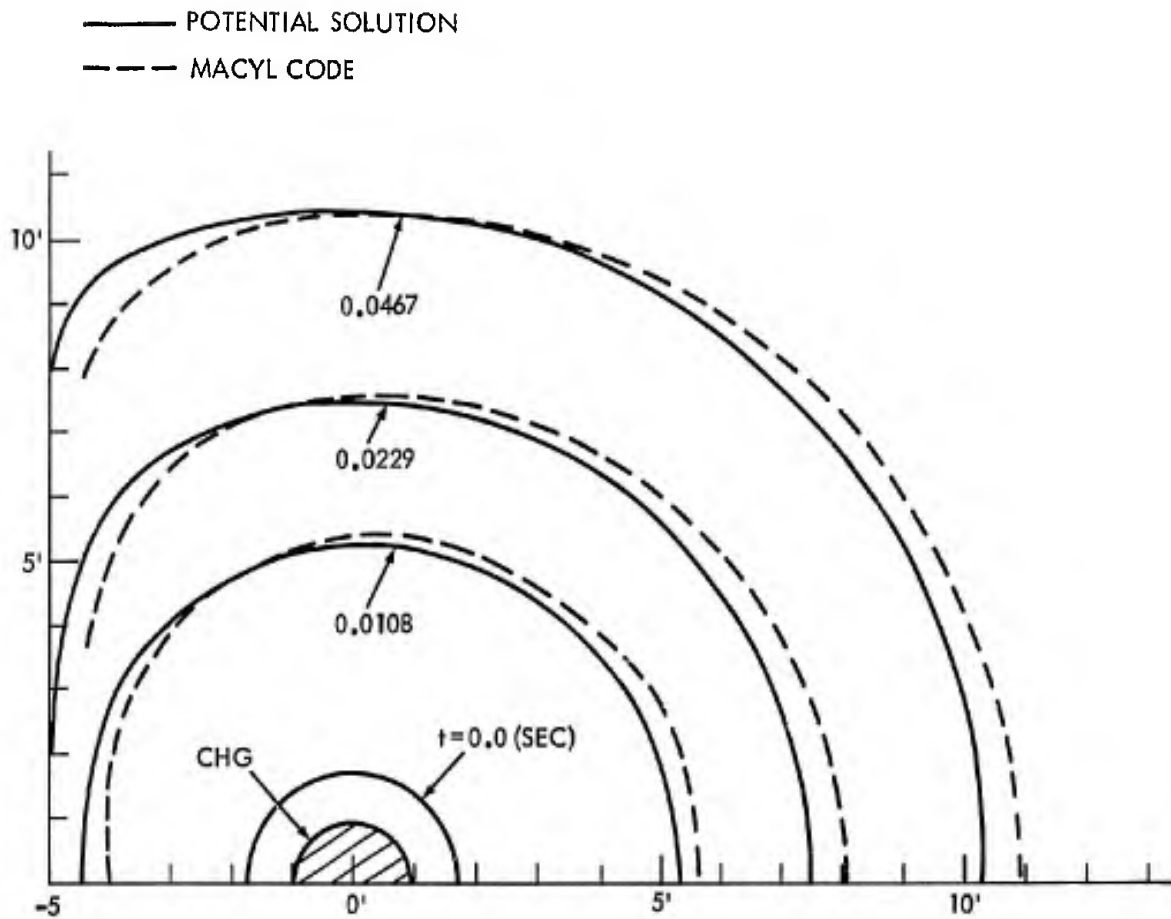


FIG. 6 COMPARISON OF CALCULATIONS MADE WITH POTENTIAL FLOW THEORY WITH CALCULATIONS BY THE MACYL CODE

The Curves Show One Quadrant Of The Bubble Expansion Of Two Simultaneously Initiated 347-lb TNT Charges Separated By 10 Feet. The Burst Depth Is 70 Feet. The Parameter Is The Time In Seconds. The Maximum Expansion Is Reached At A Time Of 0.405 Seconds.

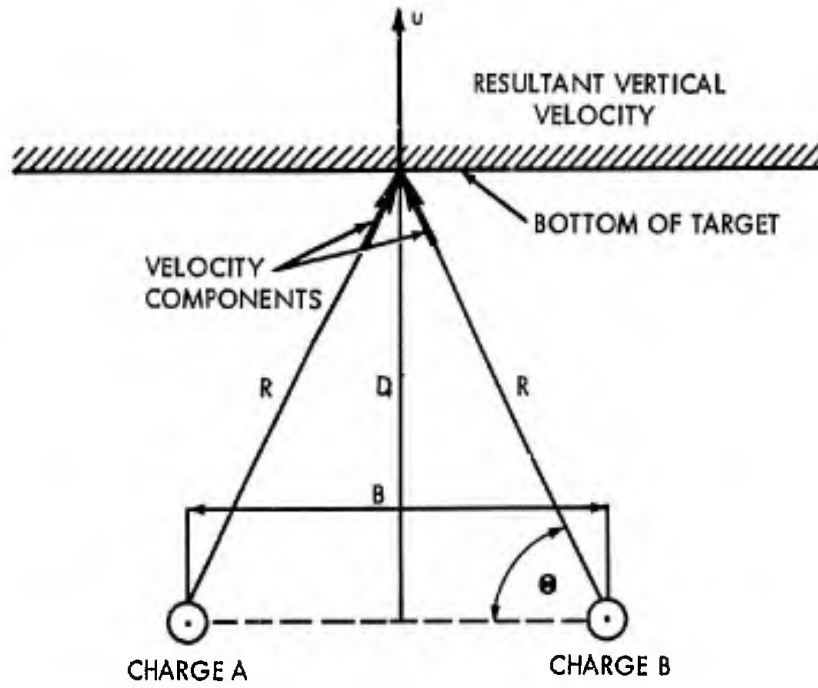


FIG. 7 EXPLOSION GEOMETRY BELOW TARGET

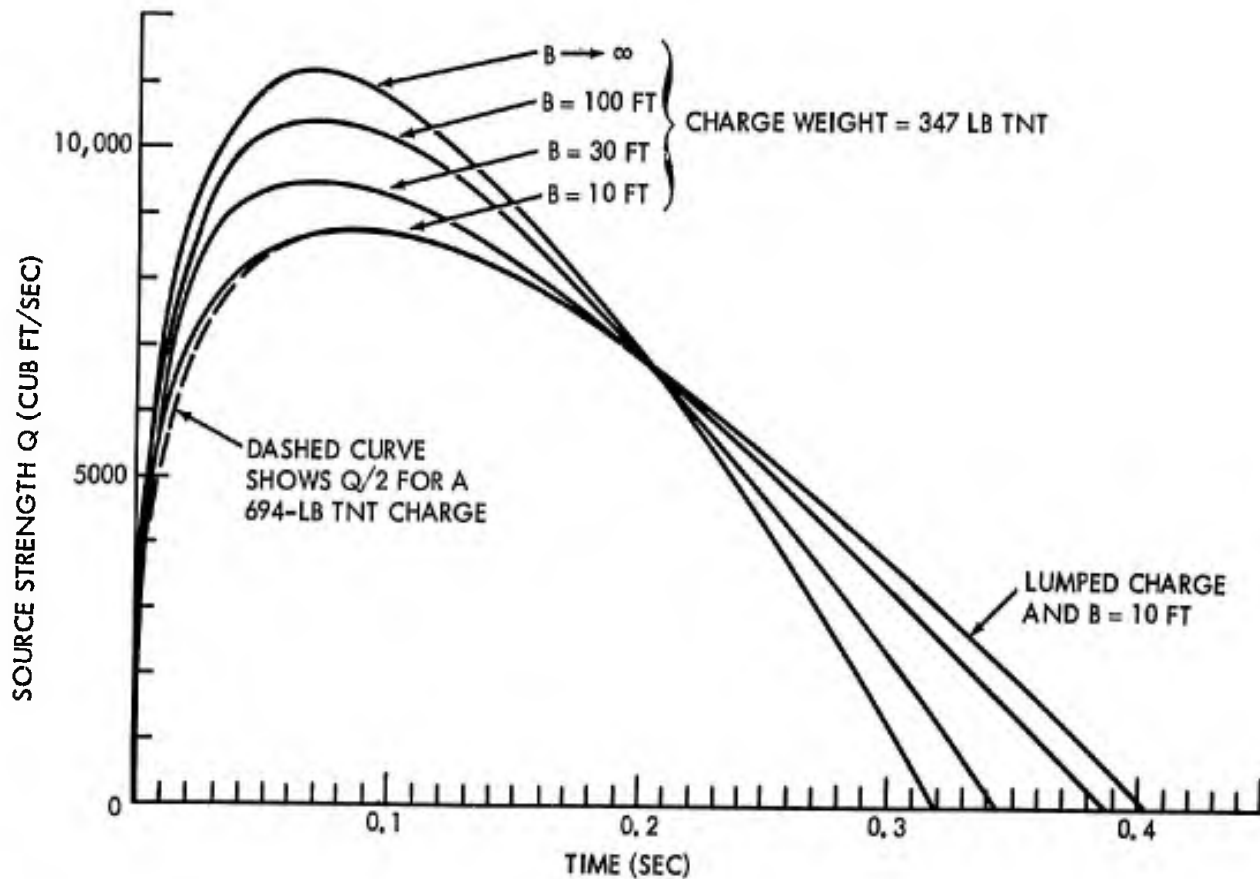


FIG. 8 SOURCE STRENGTH OF TWO INTERACTING BUBBLES AS A FUNCTION OF TIME

The Solid Curves Give The Source Strength Of One Of The Two Interacting Bubbles. The Dashed Curve Shows The Corresponding Magnitude For A Lumped Charge. The Maximum Source Strength Is Considered A Measure Of Damage Effectiveness For Whipping. The Half Period Is The Time At Which The Source Strength Vanishes. The Graph Shows That The Maximum Source Strength Decreases With Decreasing Charge Separation. For A 10-Ft Separation It Assumes The Value Corresponding To A Lumped Charge.